

# Regional Long-Period Magnitude Scales and Their Capabilities for Tsunami Warning

A. A. Gusev<sup>a, b, \*</sup> and O. S. Chubarova<sup>a, \*\*</sup>

<sup>a</sup>*Institute of Volcanology and Seismology, Far East Division, Russian Academy of Sciences, Petropavlosk-Kamchatskii, 683006 Russia*

<sup>b</sup>*Geophysical Survey, Kamchatka Division, Russian Academy of Sciences, Petropavlosk-Kamchatskii, 683006 Russia*

\**e-mail: gusev@emsd.ru*

\*\**e-mail: ochubarova@emsd.ru*

**Abstract**—The tsunami warning system in the Russian Far East employs the medium-period magnitude  $M_S(BB)$  by Vaniek–Soloviev. However, its use may lead to inadequacies and underestimates for the tsunamigenic potential of an earthquake. Specifically, this can happen in the case of a so-called tsunami–earthquake. This kind of earthquakes with a nonstandard spectrum was revealed by H. Kanamori in 1972. This problem can be overcome by using a magnitude scale that deals with longer period seismic waves. This study develops a technique for determining the magnitudes at regional distances (from 70 to 4500 km) using the amplitudes of surface seismic waves of periods of 40 and 80 s. At distances of 70–250 km, the amplitude of the joint group of shear and surface waves is used. For the new magnitudes designated  $M_S(40)$  and  $M_S(80)$ , experimental calibration curves are constructed using more than 1250 three-component records at 12 stations of the region. The magnitudes are calibrated so as to produce an unbiased estimate of the moment magnitude  $M_w$  in the critical range 7.5–8.8. The rms error of the single-station estimate  $M_w$  is around 0.27. At distances below 250 km and  $M_w \geq 8.3$ , the estimate of  $M_w$  obtained by the proposed technique becomes saturated at the level of  $M_w \sim 8.3$ , which is acceptable for operative analysis because no missed alarms arise. The technique can be used in operational tsunami warning based on seismological data. This can markedly decrease the number of false alarms.

**Keywords:** tsunamigenic earthquake, long-period calibration curve, magnitude, tsunami warning

**DOI:** 10.1134/S0001433816080065

## INTRODUCTION

Recently, for the conditions of the Russian Far East, a regional magnitude scale  $M_S(20R)$  for surface waves with a period of 20 s has been developed and successfully tested (Chubarova et al., 2010; Chebrov and Gusev, 2010; Chebrov et al., 2013). Like the  $M_S(BB)$  scale by Vaniek–Soloviev (Vaniek et al., 1962), this scale can be applied to regional distances (1–30°). Like the  $M_S(20)$  scale according to (Gutenberg, 1942), this scale uses amplitude estimates in a narrow band of periods close to  $T = 20$  s. This band is selected by a band-pass digital filter. Thus, the new scale has a strict spectral reference. For a number of reasons, the new scale is more convenient and more stable than the  $M_S(BB)$  scale that is commonly used in Russian regional seismology. The scale is well suited for operational tsunami forecasting and has already been included for several years in a corresponding automated system (Chebrov and Gusev, 2010; Chebrov et al., 2013).

The successful history of the  $M_S(20R)$  scale provided grounds for using a similar approach for waves of longer periods. The need for magnitude estimates of

this kind is associated with the fact that for the problem of tsunami forecast the longer is the wave period, the more reliable is the forecast. Cases regularly appear when the source radiation is unusually low at periods not exceeding 20 s. As a result, both the magnitude  $M_S(BB)$  and the slightly improved magnitude  $M_S(20R)$  distort and underestimate the tsunamigenic potential of earthquakes. This refers to so-called tsunami–earthquakes, for which the magnitude (in terms of  $M_w$ ) can be underestimated to 0.6–0.7 or possibly more. To avoid these cases, the threshold magnitude for tsunami alarm has to be reduced to the level of  $M_S = 7$ , which inevitably leads to unreliable estimates for danger and, as a consequence, a large number of false alarms. It is important to reduce their number without compromising the reliability of warning elaboration.

This problem can be fundamentally solved by turning to the long-period and ultra-long-period estimates of the magnitude (Kanamori and Polet, 2007). The use of long-period waves could significantly increase the reliability and validity of tsunami alarms. Ideally, one would use an estimate for the seismic moment  $M_0$  or the moment magnitude  $M_w$ ; these parameters most

adequately characterize the tsunamigenic potential of earthquakes. However, this theoretically correct concept cannot be easily implemented for local tsunamis. The confident seismological estimate of  $M_w$  for the sources of earthquakes that generate the most powerful and catastrophic tsunamis ( $M_w = 8.5-9.5$ ) requires the use of oscillations with periods of up to 500 s or more. These approaches are well known. For example, Lee et al. (2012) use records at distances of  $15-20^\circ$  for this purpose. It was shown on three examples that the record in this case allows one to determine both  $M_w$  and the seismic moment tensor. Here, waves with periods of up to 500 s were analyzed to ensure that the value of  $M_w$  for earthquakes with  $M_w \geq 9$  is determined adequately and without any substantial underestimation.

For operational estimates, one can do without determining the tensor structure of the source, dealing only with magnitude-type estimates. The long-period magnitude in surface waves is a well-developed concept. For the teleseismic case, Brune and King (1967) introduced the concept of “mantle magnitude” on the basis of waves with periods of around 100 s. This approach was further developed by Prozorov et al. (1977) for a wider range of periods from 50 to 300 s. Okal and Talandier (1989) proposed a similar magnitude  $M_m$ , which was calculated from Fourier spectra in the range of periods from 30 to 300 s; by definition,  $M_m$  is directly associated with  $\log M_0$ , and the distances considered were above  $20^\circ$ .

However, even magnitude estimates have a problem with the generation of a tsunami alert for coastal points directly in front of the earthquake source. One of these difficulties is that the amplitude estimates on the time periods mentioned above (300–500 s) require a sufficient time reserve. Let us consider a conditional but realistic example. If the distance between the station and the axis of the extended source with  $M_w = 9$  is in the range from 80 to 150 km, the tsunami wave runup time can be 10–15 min (600–900 s), and the alert should be issued at least after 300 s or, more preferably, 200 s of the initiation of the source process. At this time, the waves with periods of 300–500 s had not been formed yet because the break in the source with  $M_w = 8.8-9.2$  lasts longer than 200 s. For example, the source formation time for the Sumatra earthquake of December 26, 2004 ( $M_w = 9.3$ ) is around 550 s.

Now, we consider a simpler case of a source with a size of  $\sim 220$  km with  $M_w = 8.3$ , when the period of a wave with a length of about the source size is  $\sim 70$  s. This wave should reach the station; then, the station should record at least one complete wave period (or better, one and a half period). Assuming that the speed of the wave (transverse or surface) is 3 km/s and the epicentral distance is 150 km, we obtain a time loss before the signal processing of around 160 s. This allows us to expect that the processing could be performed normally within 200–250 s. However, if  $M_w > 8.3$ , performing the given

program will still estimate the magnitude as 8.3–8.5 or less. The values of  $M_w$  are underestimated relative to the true value for two reasons: (1) the spectrum limitations already discussed above play a role and (2) the waves from the remote parts of the source do not have time to reach the receiver for a source with  $M_w = 8.5$  or more. This means that the seismological method of magnitude estimation for a given time limit of 200–300 s and  $M_w > 8.3-8.5$  yields “saturated” estimates in the range  $M_w = 8.3-8.5$ . Therefore, accurately determining the magnitude under given time limitations is simply an unsolvable problem.

However, from the practical point of view, if the magnitude estimation technique yields an estimate bounded for  $M_w > 8.3-8.5$  by the upper threshold in the range  $M = 8.3-8.5$  and suitable at lower magnitudes, this should not be an obstacle for these techniques to be used in operational activities because all practical algorithms of tsunami warning produces alerts at significantly lower thresholds (normally, in the range  $M = 7.5$ ). This simply means that if the estimate is in the range  $M_w \approx 8.3-8.5$  and obtained at the station near the source, it should be considered an operational minimal estimate and be corrected later using data of more remote stations. An example of this correction can be found in (Lee et al., 2012).

The existing Russian practice of primary use of waves with a period of 20 s needs to be urgently revised. To produce a tsunami alert at the nearest coast in reasonably short time, one has to seek a workable, albeit nonstrict, compromise. In view of the above considerations, the present study considers the use of operational procedures in a limited range of periods from 30 to 100 s. This concept is implemented in practice by using signals at the output of band-pass filters with axial frequencies corresponding to periods of 40 and 80 s. The bandwidth of the filters is  $2/3$  of an octave; thus, these filters cover (at the level of  $-3$  dB) ranges of periods from 32 to 50 and from 64 to 100 s.

We discuss the extent to which this approach can improve the alert formation specifically for tsunami–earthquakes. At low magnitudes (for example,  $M_S = 7-7.3$  and  $M_w = 7.7-8$ ), the use of a range of periods up to 100 s comparable with the source length of earthquakes can obviously and significantly improve the results in comparison with the use of variants of the  $M_S$  scale. These earthquakes are well known (Kanamori and Polet, 2007). Data on more powerful tsunami–earthquakes are fragmentary. The best known tsunami–earthquake is that of June 6, 1896, with  $M_w = 8.2$  and  $M_S = 7.4$  (Abe, 1989). This tsunami–earthquake is known for its very weak perceived shaking (with periods of 0.3–2 s) quakes on the coast; its radiation in the range of periods of 20 s was also anomalously low. This case should not be missed as dangerous according to the new technique. In general, in most cases, one can expect a substantial gain from estimating the magni-

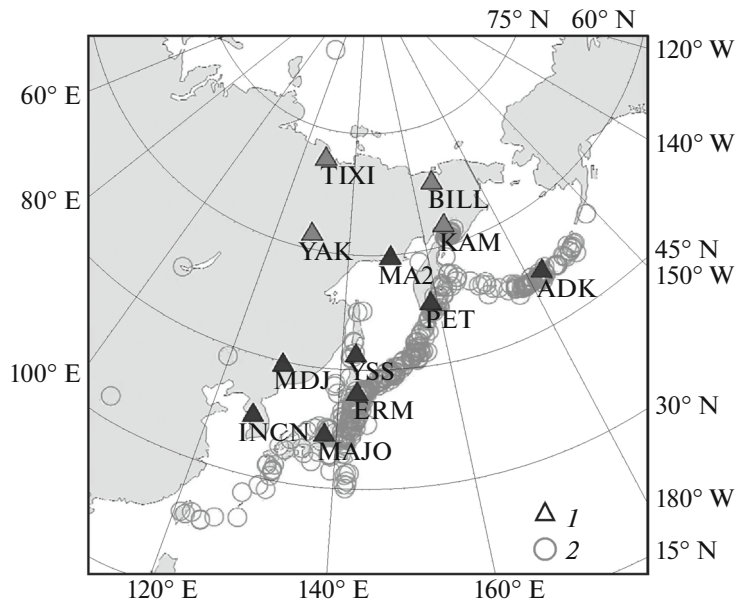


**Fig. 1.** Map of the epicenters of earthquakes in the northwest Pacific (1) and digital seismic stations (2) used to construct calibration functions.

tude of waves with periods of 30–100 s instead of waves with a period of 20 s accepted presently.

It is important to make the following terminological reservation. At small (70–250 km) epicentral distances, after the transverse wave arrival, the regional records actually involve a single wave packet, which can be regarded as an inseparable group of transverse and surface waves. For brevity, this group is called a surface wave, although this is terminologically incorrect. It is the amplitude of this group of waves that is used by us to estimate the magnitude.

### GENERAL APPROACH

In this paper we construct a magnitude scale with respect to surface waves with periods of 40 and 80 s. At epicentral distances of less than  $3^\circ$ , the regional records actually involve an inseparable group of transverse and surface waves. To construct this scale, we experimentally determine the standard distance trend (calibration function) for the amplitudes of surface wave in regional records. The amplitudes are measured after filtration in a narrow range of periods in bands with axial periods of 40 and 80 s (with frequencies of 0.025 and 0.0125 Hz and a bandwidth of around  $2/3$  of an octave). The calibration functions are constructed through the normalization of observed amplitudes with the help of theoretical spectral functions, the values of which are calculated for each event on the basis of the values of the moment magnitude  $M_w$  of the GCMT catalog (<http://www.iris.edu/dMs/wilber.htm>) and the frequency of spectral bend (“corner-frequency”) estimated from  $M_w$  on the basis of known correlations. For waves of periods 40 and 80 s, the calibration functions

are found with an acceptable accuracy. The absolute level in the formula for calculating the magnitude is taken so that the values of new magnitude ( $M_S(40)$  and  $M_S(80)$ ) are numerically close to  $M_w$ . This makes it possible to obtain a suitable operational estimate for  $M_w$  up to  $M_w = 8.5–8.7$  even in conditions of a rare seismic network. For higher magnitudes  $M_w = 8.8–9.6$ , the resulting values of  $M_S(40)$  and  $M_S(80)$  are lower estimates for  $M_w$ , which is suitable for tsunami warning services.

### INITIAL DATA

The initial data used in this study involve records of 433 earthquakes in the northwestern Pacific from 1993 to 2009 obtained at 12 broadband digital seismic stations (PET, YSS, MA2, YAK, KAM, ADK, TAXI, BILL, MDJ, INCN, ERM, and MAJO) in the northwestern part of the Pacific Ocean (Fig. 1): a total of more than 1250 three-component records of BH-channels in the range of epicentral distances of  $0.7–40^\circ$ . The digital records of earthquakes were taken from the IRIS DMC archive and the tsunami database of the Kamchatka branch of the Geophysical survey, Russian Academy of Sciences (RAS). The depth of earthquake sources is up to 70 km. We consider only the earthquakes that have an estimate for the moment magnitude  $M_w$  in the GCMT catalog (<http://www.globalcmt.org/CMTsearch.html>) (see Fig. 1). The range of magnitudes of the earthquakes considered by us is 4.7–8.3. The original digital records were processed by the DIMAS program (Droznin and Droznina, 2010).

## CONSTRUCTION OF CALIBRATION FUNCTIONS

To construct calibration functions of new regional magnitudes  $M_S(40)$  and  $M_S(80)$ , we significantly modified the technique used earlier for the regional magnitude scale  $M_S(20R)$  (Chubarova et al., 2010). To construct the scale  $M_S(40)$ , we analyzed the distance dependence of maximum displacement amplitudes of the shift  $A$  in surface waves passed through a bandpass filter with an axial frequency of 0.025 Hz. We used a physically realizable (causal) fourth-order Butterworth filter with cutoff frequencies of 0.03125 and 0.02 Hz (periods of 32–50 s). Similarly for the  $M_S(80)$  scale, the axial frequency of the filter was 0.0125 Hz and the cutoff frequencies were 0.15625 and 0.01 Hz (periods of 64–100 s). The filters were applied to the displacement signal obtained by inverse filtering of digital records of the BH velocigraph. This operation is not necessary: the bandpass filtering can be applied equally well directly to the velocigraph output (the record of velocity). The relevant small phase distortions are insignificant for the problem of magnitude classification. Nevertheless, at the stage of scale construction, we found it necessary to eliminate them.

The maximum amplitudes were measured in a 600-s time window after the  $S$ -wave arrival: ( $t_S, t_S + 600$  s), where  $t_S$  is the  $S$ -wave arrival time. The maximum values in each of the three components were measured at independent time instants. One example of a record of earthquake and measurements is shown in Fig. 2. To control the measured maxima of specific waves, we analyzed the relationship between the measurement time of the maximum amplitude of surface waves  $t_L$  (the time is counted from the source time  $t_0$ ) and the epicentral distance  $\Delta$ . It should be noted that the phase shift in the bandpass filter makes the measured time  $t_L$  apparent and lagging behind from the ideal time (for the case of zero phase shift) by almost one and a half period (the delay is  $dt_f \approx 60$  for a period of 40 s and  $dt_f \approx 120$  s for a period of 80 s). We used this technique because it is prospective for further use in real time. In this case, a practically convenient filtering algorithm requires a physically realizable filter (commonly, a recursive digital filter). The resulting plots of  $t_L(\Delta)$  for the vertical component of oscillations are shown Fig. 3. These plots were used to construct a straight-line surface (Rayleigh) wave travel time function. The observed velocities (actually, group velocities) are 2.95 km/s for  $T = 20$  s (Chubarova et al., 2010), 3.5 km/s for  $T = 40$  s, and 3.6 km/s for  $T = 80$  s. To calculate the magnitude at a given station on the basis of  $M_S(20R)$ , we used the rms value of maxima of amplitudes of the three components recorded at independent time instants. Hereafter, the rms amplitude is denoted as  $A$ .

As usual, we assumed that the magnitude  $M_S(T)$  for the period  $T$ , which is denoted simply as  $M_S$  for brev-

ity, is determined by the formula  $M_S = \log A - \sigma(\Delta)$  (where  $\Delta$  is the epicentral distance); here, it is convenient to write the function  $\sigma(\Delta)$  as

$$\sigma(\Delta) = C_1 - \tau(\Delta). \quad (1)$$

The calibration function  $\tau(\Delta)$  (i.e., the function of amplitude attenuation with distance for the period  $T$ ) was chosen by repeating several iterations of the following steps.

(1) Using the current variant  $\tau^{(i)}(\Delta)$ , where  $i$  is the number of iteration, all amplitudes are brought to a given reference distance  $\Delta_0$  to obtain the reduced amplitudes

$$\log A_0^{(i)} = \log A - \tau^{(i)}(\Delta) + \tau^{(i)}(\Delta_0). \quad (2)$$

(2) For each given earthquake, its value  $M_w = M_w(\text{GCMT})$  is used to find the “calculated” reduced amplitude  $A_0^{(C)(i)}$  of the surface wave of period  $T$  at distance  $\Delta_0$ , assuming it to be proportional to the value of the source spectrum at a fixed frequency  $f_T = 1/T$ . This step consists of the follow these stages:

(2.1) on the basis of  $M_w(\text{GCMT})$ , estimate the earthquake corner-frequency  $f_c$ , assuming that  $f_c$  and  $M_w$  are related according to the hypothesis of source similarity:

$$\log(f_c^{(i)}) = -1/2(M_w - M_w^{(i)}) + \log f_T. \quad (3)$$

Here, parameter  $M_w^{(i)}$  means a typical value of  $M_w$  for the case of earthquake with  $f_c = f_T$ . Its exact numerical value (in the range between 7.5 and 8) is determined by try and error and corrected at each iteration;

(2.2) for the model source with a corner-frequency  $f_c$  and magnitude  $M_w$ , specify a spectral function for calculating spectral corrections with the help of Brune’s generalized formula

$$a(f_T, f_c)^{(i)} = \log \frac{1}{1 + (f/f_c)^{\gamma^{(i)}}}. \quad (4)$$

Here, the spectral parameter  $\gamma^{(i)}$  (in the range between 1.3–2) is corrected in each iteration;

(2.3) substituting the value of frequency  $f = f_T$  in (4), estimate the level of source spectrum of the current event at the frequency  $f_T$  as

$$\log A_0^{(C)(i)} = 1.5M_w + C_2 + a(f_T, f_c)^{(i)}, \quad (5)$$

where  $C_2$  is an insignificant constant. It should be explained that  $(1.5M_w + C_2)$  is the logarithm of source spectrum for  $f = 0$ . The value of  $A_0^{(C)(i)}$  can be simultaneously interpreted as the amplitude of peak at the output of a bandpass filter with a fixed width and axial frequency  $f_T$ .

(3) For earthquake population, the dependence of  $\log A_0$  on  $\log A_0^{(C)(i)}$  should ideally be a constant function:  $\log A_0 = \log A_0^{(C)(i)} + C_3$ . The systematic devia-

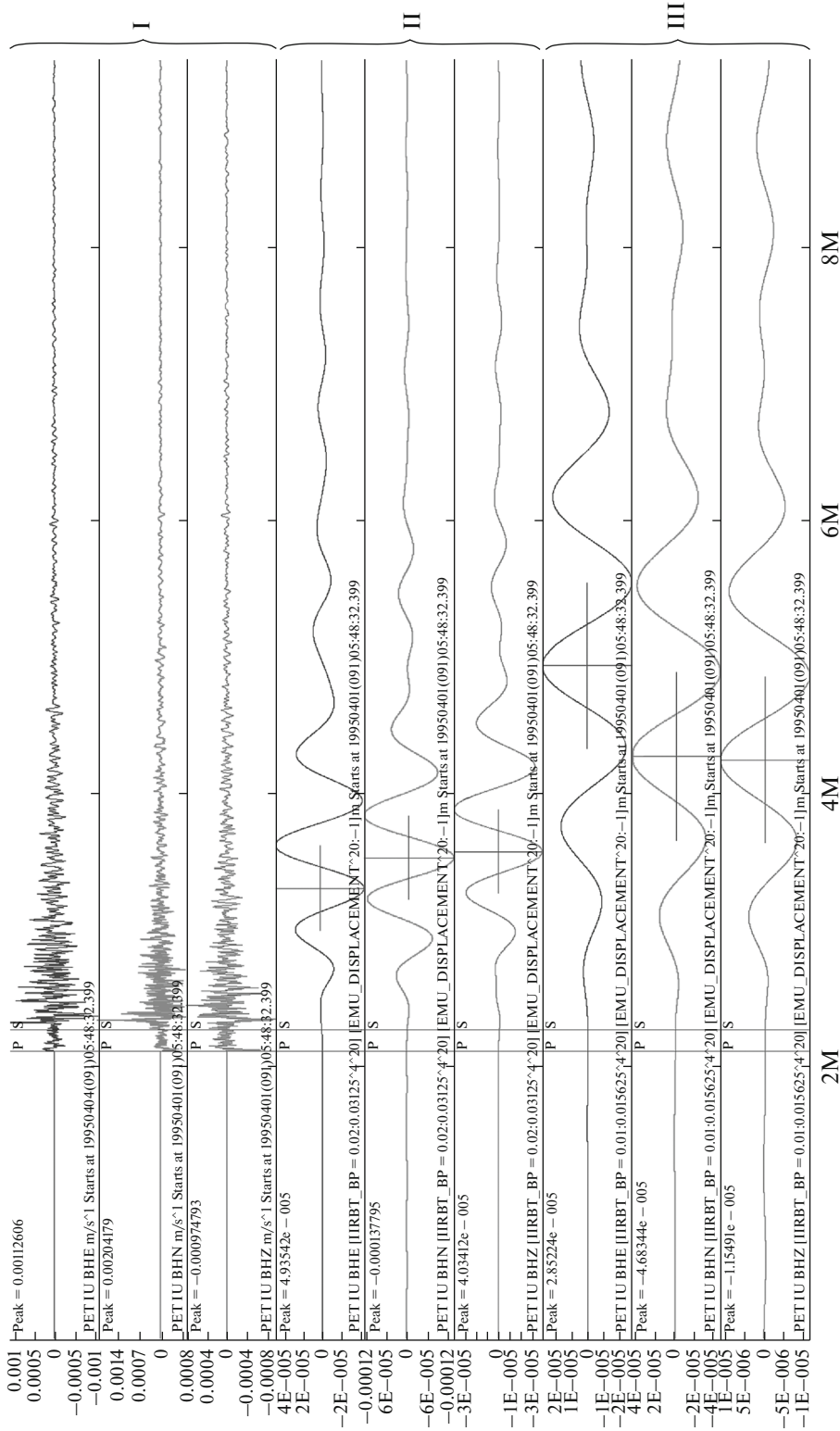


**Fig. 2.** Example of a record of an earthquake and measurements in the DIMAS dialog window: (I) velocigraph signals on the components (top to bottom) BHE, BHN, and BHZ; (II) the result of bandpass filtering of the displacement signal for a period of 40 s; and (III) same as (II) except for a period of 80 s. The vertical lines indicate the arrival times of P and S waves and the measurement times of the amplitudes of filtered surface waves. The step of time marks is 2 min. The amplitudes of vertical channels (bottom) are 974 mm/s, 40 mm/s, and 11 mm/s for groups I, II, and III, respectively. The amplitudes of horizontal channels are comparable.

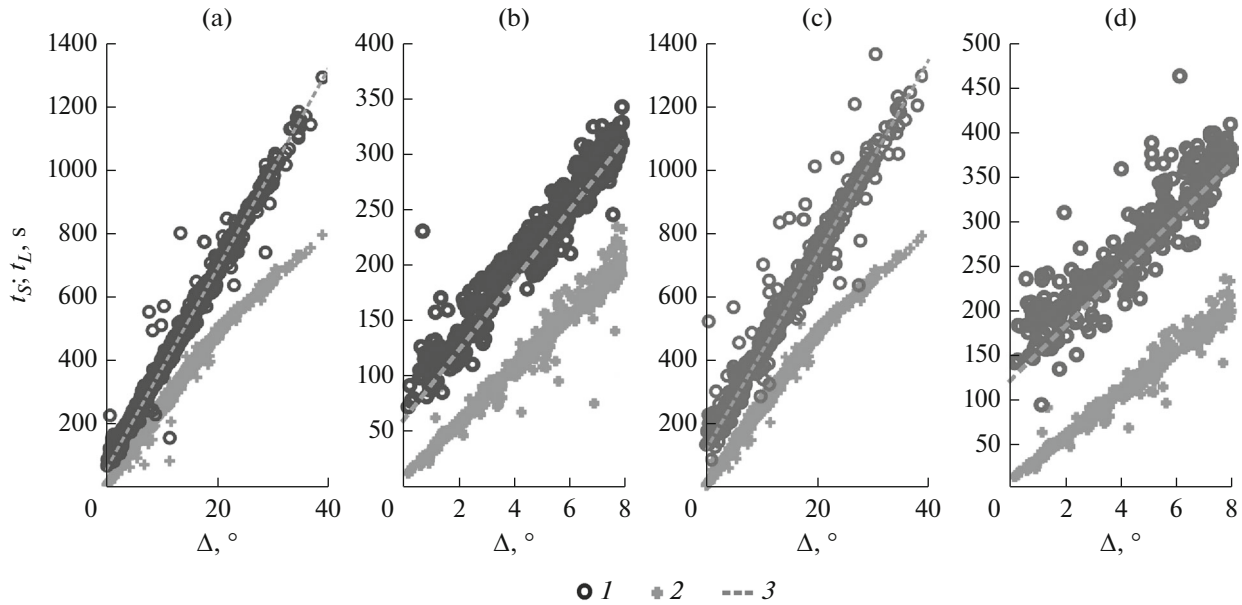


**Fig. 3.** Dependence of  $t_L$  (the measurement time of the amplitude of displacement) on  $\Delta$  for vertical components (1) at the output of the actually used bandpass filter: (a) full range of times and distances for a period of 40 s; (b) only small epicentral distances for a period of 40 s; and (c, d) same as (a) and (b) except for a period of 80 s. (2)  $S$ -wave arrivals taken from the record; (3) straight-line travel time curves of Rayleigh waves with group velocities: 3.5 km/s for  $T = 40$  s (a, b) and 3.6 km/s for  $T = 80$  s (c, d). The time is counted from the origin time  $t_0$ .

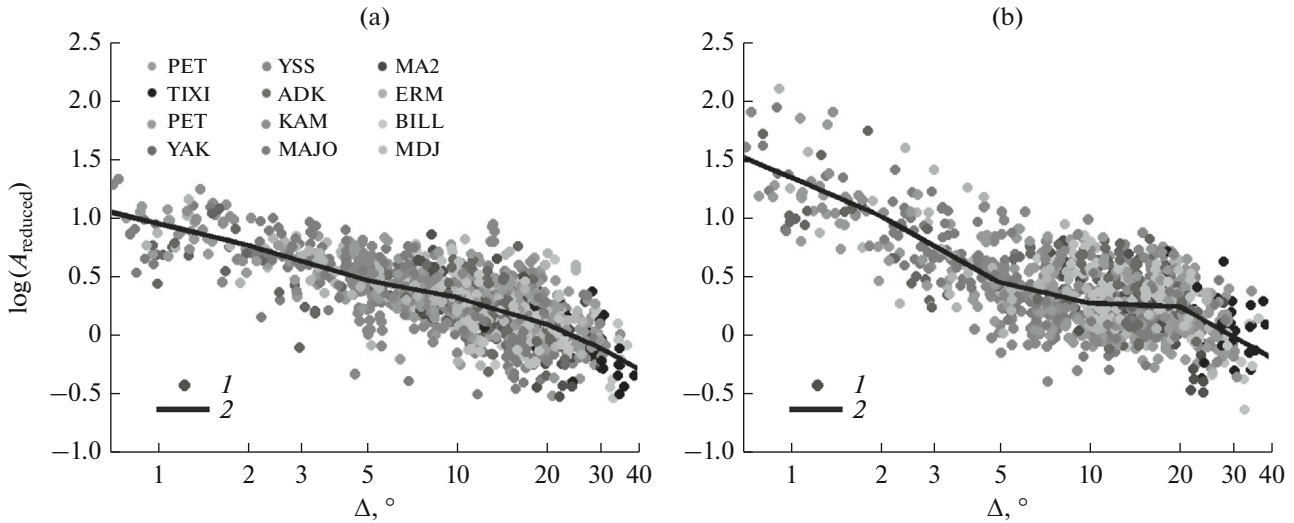


**Fig. 4.** Normalized station amplitudes for magnitudes  $M_s(40)$  (a) and  $M_s(80)$  (b): (1) observed data (rms value of the three components) and (2) calibration function for the magnitude  $M_s(T)$ .

tions from this relation observed for the current iteration can be reduced by modifying the parameters  $M_{w0}$  and  $\gamma$ . After several iterations, we found the desired estimates for these parameters in our case. The final estimates are  $M_{w0} = 7.5$  for  $T = 40$  s and  $M_{w0} = 7.9$  for  $T = 80$  s; in both cases,  $\gamma = 1.5$ .

(4) The trend of residual differences  $\log A_0 - \log A_0^{(C)}$  in function  $\Delta$  should ideally yield a constant function. The actual deviations from a constant function can be reduced by modifying the function  $\tau(\Delta)$ , as conducted by us. This modification would be followed by another

cycle of iterations (steps 2 and 3); however, it turned out that there is no need for that: the estimates of  $M_{w0}$  and  $\gamma$  remain stable when  $\tau(\Delta)$  is adjusted.

The constant  $C_1$  was chosen so that the new magnitudes  $M_s$  were numerically close to the moment magnitude  $M_w$  in the range from 7.0 to 8.4. For higher magnitudes, no data were available. For lower magnitudes, the value of  $M_w$  on the average was always higher than  $M_s(T)$ . The result of this iterative search is stable and independent of the initial approximation. The new calibration functions are shown in Fig. 4, and the

scatter of residuals after the iterative search is shown in Fig. 5. The final variants of functions  $\tau(\Delta)$  are given below (through the nodal points).

NEW SCALES

We describe the recommended calibration functions to determine the magnitudes  $M_S(40)$  and  $M_S(80)$  and the procedure of their use in calculations.  $M_S(40)$  and  $M_S(80)$  are determined by the formulas

$$M_S(40) = \log(A) - \tau_{40}(\Delta) + 4.670, \quad (6)$$

$$M_S(80) = \log(A) - \tau_{80}(\Delta) + 5.115, \quad (7)$$

where  $\tau_{40}(\Delta)$  and  $\tau_{80}(\Delta)$  are the new calibration functions that are numerically determined according to the procedure described below;  $\Delta$  is the epicentral distance (in degrees),  $0.7^\circ < \Delta < 40^\circ$ ;  $A$  is the rms value (over three channels) of the maximum (“2A”/2) amplitude of displacement at the output of the above-described causal digital filter ( $\mu\text{m}$ ) in the time window ( $t_S, t_S + 600$  s); and  $t_S$  is the  $S$ -wave arrival time. The maximum amplitude corresponds to either a surface wave or (normally, at  $\Delta \leq 3^\circ$ ) an inseparable group of transverse and surface waves. The calibration functions  $\tau_{40}(\Delta)$  and  $\tau_{80}(\Delta)$  are given by their nodal values for the set of nodes  $\Delta$  (see the table). This procedure is supposed to be used for sources with depths of less than 70 km.

The accuracy of the resulting estimates can be estimated from fitting errors of calibration functions (see Fig. 4). The corresponding standard deviation is 0.20 for  $M_S(40)$  and 0.25 for  $M_S(80)$ . Also, we estimated the prediction error of  $M_w$  from the principle  $M_w = M_S(40)$  for  $M_w > 7$  or  $M_w = M_S(80)$  for  $M_w > 7.2$ . The average error is less than 0.03 and the standard deviation is 0.25–0.28. Thus, for large magnitudes,  $M_S(40)$  and/or  $M_S(80)$  are good operational estimates of  $M_w$  even in the case of a single station. This possibility was checked up to  $M_w = 8.3$ . For even higher magnitudes, the estimates of this kind are on the average slightly below the true values (the expected distortion is up to  $-0.2$ – $-0.3$  units of  $M$  for  $M_w$  of around 9.2), which is suitable for operational work. The theoretical average relationship of the new magnitudes with  $M_w$  is shown in Fig. 6. For the case of operational work, it should be

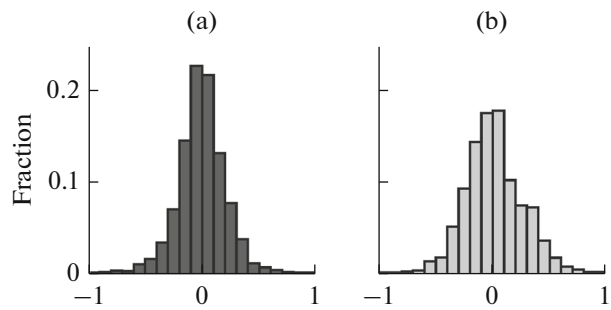


Fig. 5. Distribution of residuals in individual normalized amplitudes for the magnitudes  $M_S(40)$  (a) and  $M_S(80)$  (b).

explained that it makes sense to take the larger of the two values of the above-discussed magnitudes as an estimate of  $M_w$ .

PROSPECT OF NEW SCALES IN REAL TIME

The only element of the above-described technique that cannot be directly implemented in the real-time mode is the use of inverse filtering for the transition from velocigram to displacement recording. This question was analyzed in detail for the case of  $M_S(20)$ . For a record with a narrow band of frequencies, the trivial relation for the sinusoidal signal

$$A = V/(2\pi/T), \quad (8)$$

where  $A$  and  $V$  are the amplitudes of displacement and velocity, respectively, are satisfied with a very acceptable accuracy for peak amplitudes of wave groups as well. This fact was checked for several dozens of records at the output of filters used by us and was well confirmed. Thus, in the real-time mode, the inverse filtering can be replaced by the simple approach described above: apply a bandpass filter directly to the velocigraph signal, measure its peak value  $V$ , and then determine  $A$  from formula (8).

In addition to the amplitude, the operational estimate of the magnitude requires at least rough estimates of the epicentral distance. This is commonly achieved by using the delay of  $S$ -wave arrival relative to the  $P$ -wave arrival ( $S-P$ ). However, near large sources, it is often impossible to fix (especially in real time) the  $S$ -wave arrival because the length of the

Nodal points of calibration functions  $\tau_{40}(\Delta)$  and  $\tau_{80}(\Delta)$  of magnitude scales on surface waves  $M_S(40)$  and  $M_S(80)$  for the set of nodal values of epicentral distance

Parameters	Epicentral distance ( $\Delta$ ), $^\circ$						
	0.7	2	5	10	20	30	40
$\log(\Delta)$	-0.1549	0.3010	0.6990	1.0000	1.3010	1.4771	1.6021
$\tau_{40}(\Delta)$	1.06	0.78	0.48	0.33	0.09	-0.11	-0.28
$\tau_{80}(\Delta)$	1.53	1.03	0.46	0.28	0.25	0.00	-0.17

For intermediate values of  $\Delta$ , the functions  $\tau_{40}(\Delta)$  and  $\tau_{80}(\Delta)$  should be calculated using a linear interpolation with respect to the argument  $\log(\Delta)$ .

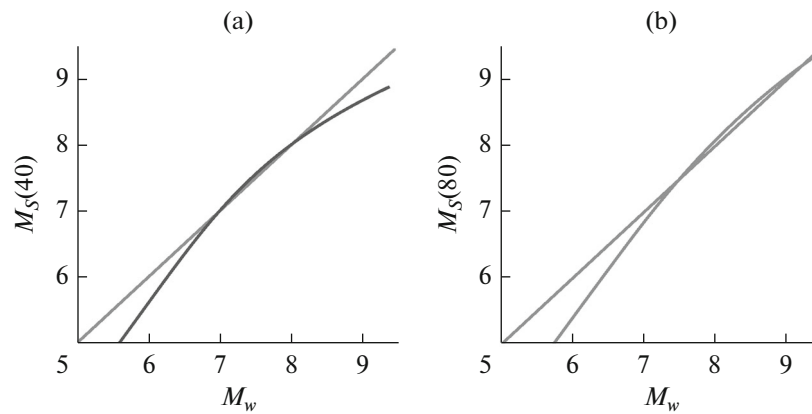


Fig. 6. Theoretical dependence of new magnitudes  $M_S(40)$  (a) and  $M_S(80)$  (b) on the moment magnitude  $M_w$ .

source process can easily exceed  $S-P$ . In this case, the arrival of  $S$  waves is overlapped by energetic  $P$  waves from later stages of the source development, and the arrival turns out to be completely noisy. This difficulty can be overcome through the use of the surface-wave signal. It follows from Fig. 3 that the delay in the maximum in the long-period surface wave can yield a sufficiently stable rough estimate for the distance. Although the time count in Fig. 3 goes from  $t_0$ , it is clear that this conclusion remains true for the practically basic case when the time count starts from the  $P$ -wave arrival. Figure 2 demonstrates that if the arrival time of the maximum is counted with respect to the maximum of the envelope (the amplitude of analytical signal) rather than with respect to the time of the actual amplitude maximum, the travel time accuracy (and, therefore, the estimate of  $\Delta$ ) can be significantly improved.

## DISCUSSION

Talandier and Okal (1992) extended the use of the long-period magnitude  $M_m$  by surface waves to the regional case. They checked the principal possibility of such a procedure in a range of distances of  $1.5-15^\circ$  (mainly, the range  $2.5-15^\circ$  was considered). The practical implementation of the Okal–Talandier technique (Schindel e et al., 1995) indicated that the time of  $P$ -wave arrival before the algorithm operation was 15 min, which is unacceptably late for the Far East coasts. It should be noted that the study mentioned above, like the present study, used both the vertical and horizontal components of records. It is of interest to compare the two studies in terms of accuracy. The standard deviation for the estimate  $\log M_0$  in (Schindel e et al., 1995) was 0.29 for the case of shallow earthquakes (by a single station). The scatter estimates for  $M_w$  are obtained from multiplying by  $2/3$ , which yields 0.19. Our estimate of the scatter was slightly worse, which is understandable because a limited bandwidth was used. The novelty of the present study is largely in the fact that we constructed and tested an estimate (or,

a lower estimate for  $M > 8.3$ ) of the long-period magnitude at extremely low (up to  $0.7^\circ$ ) epicentral distances.

As an alternative to the approach developed by us one can consider the broadband magnitude of *drop*:  $S$ . Tsuboi by  $P$ -waves  $M_{wp}$  (Tsuboi et al., 1995). Even if one uses the first 120 s of the record, this magnitude on the average gives a good estimate of the tsunamigenic potential. However, Hirshorn and Weinstein (2011) noted that  $M_{wp}$  can underestimate the potential of tsunami–earthquakes. This problem was partially corrected by researchers of P. Bormann’s group (Bormann and Wylegalla, 2005; Bormann et al., 2006) by summing the amplitudes on a time interval of suitable length. However, the minimum epicentral distance necessary to use these techniques is 550 km.

The technique proposed in this paper for estimating the long-period magnitude (and, simultaneously, the tsunamigenic potential) of earthquakes according to data of a single station is of practical interest for tsunami warning services. The technique is especially important for island coasts or sparsely populated lands. In this case, it may well prove that there is only a single station at which records of surface waves managed to arise within a temporal window of acceptable length (200–300 s). In these cases, the more “advanced” approaches to describing the tsunamigenic potential of the source (such as the operational estimate of the seismic moment tensor) cannot be implemented. At the same time, the magnitude approach retains its applicability.

For small (up to 250–300 km) distances and higher magnitudes  $M_w$ , the approach developed by us underestimates the magnitude for reasons explained in the Introduction. At distances exceeding 300 km, the values of  $M_S(40)$  and  $M_S(80)$  can be used to obtain a low-distorted estimate of  $M_w$  in the most important range  $M_w = 7-8.8$ ; at larger values of  $M_w$ , these cases are characterized by a systematic underestimation, reaching  $-0.2-0.3$  for  $M_w$  of around 9.2. This is an inevitable consequence of the limitations on the frequency band.

## CONCLUSIONS

Using data of a sufficiently large amount (more than 1250 records at 12 stations), we have successfully constructed regional long-period magnitude scales  $M_S(40)$  and  $M_S(80)$  for the conditions of the Russian Far East. According to data of a single station, the rms error of this estimate is 0.20–0.25. The operational estimates of the magnitude are needed primarily for tsunami warning services. The use of waves of periods of 40 and 80 s can substantially improve the technique of prediction of dangerous tsunami. An important parameter for tsunami prediction is the moment magnitude  $M_w$ . Using the values of  $M_S(40)$  and  $M_S(80)$ , one can obtain a low-distorted estimate of  $M_w$  in the most important range 7–8.8; larger values of  $M_w$  a slight systematic underestimation is possible, which is insignificant in practice. The rms error of this estimate of  $M_w$  at a single station reaches 0.28. Here, the time required for signal processing reaches 4–5 min for epicentral distances of up to 300 km (see Fig. 3), which is suitable with respect to time requirements for issuing tsunami alarms.

## ACKNOWLEDGMENTS

This study was conducted in the Geophysical Survey of the Kamchatka Division of the Russian Academy of Sciences and supported (in terms of the technique, calculations, and estimates, except for the collection and processing of seismogram data) by the Russian Science Foundation, project no. 14-17-00621. The authors are grateful to S.A. Vikulina for her technical assistance and appreciate the Incorporated Research Institutions for Seismology (IRIS) consortium for providing us with access to digital records.

## REFERENCES

- Abe, K., Quantification of tsunamigenic earthquakes by the  $M_t$  scale, *Tectonophysics*, 1989, vol. 166, pp. 21–34.
- Bormann, P., Wylegalla, K., and Saul, J., Broadband body-wave magnitudes  $mB$  and  $mBC$  for quick reliable estimation of the size of great earthquakes, in *USGS Tsunami Sources Workshop 2006*. [http://spring.msi.umn.edu/USGS/Posters/Bormann\\_et\\_al\\_poster.pdf](http://spring.msi.umn.edu/USGS/Posters/Bormann_et_al_poster.pdf).
- Bormann, P. and Wylegalla, K., Quick estimator of the size of great earthquakes, *EOS, Trans. Am. Geophys. Union*, 2005, vol. 86, no. 46, p. 464.
- Brune, J. and King, C.-Y., Excitation of mantle Rayleigh wave of period 100 s as a function of magnitude, *Bull. Seismol. Soc. Am.*, 1967, vol. 57, pp. 1355–1365.
- Chebrov, D.V. and Gusev, A.A., Automatic real time parameter determination of tsunami earthquakes in the Far East of Russia: Algorithms and software, *Seism. Instrum.*, 2011, vol. 47, no. 3, pp. 223–240.
- Chebrov, D.V., Chebrov, V.N., Vikulina, S.A., and Ototyuk, D.A., Estimating the magnitudes of strong earthquakes in the *Petropavlovsk* regional data processing center within the Tsunami Warning Service, in *Problemy kompleksnogo geofizicheskogo monitoringa Dal'nego Vostoka Rossii: Trudy Chetvertoi nauchno-tehnicheskoi konferentsii, g. Petropavlovsk-Kamchatskii, 29 sentyabrya–5 oktyabrya 2013 g.* (Problems in the Complex Monitoring of the Russian Far East: Proceedings of Scientific and Practical Conference, Petropavlovsk-Kamchatsky, September 29–October 5, 2013), Chebrov, V.N., Ed., Obninsk: GS RAN, 2013, pp. 299–303.
- Chubarova, O.S., Gusev, A.A., and Vikulina, S.A., The 20-second regional magnitude  $M_S(20R)$  for the Russian Far East, *Seism. Instrum.*, 2011, vol. 47, no. 3, pp. 241–245.
- Droznin, D.V. and Droznina, S.Ya., Interactive DIMAS program for processing seismic signals, *Seism. Instrum.*, 2011, vol. 47, no. 3, pp. 215–224.
- Gutenberg, B., Amplitudes of surface waves and magnitude of shallow earthquakes, *Bull. Seismol. Soc. Am.*, 1945, vol. 35, pp. 3–12.
- Hirshorn, B. and Weinstein, S., Earthquake source parameters, rapid estimates for tsunami warning, in *Extreme Environmental Events: Complexity in Forecasting and Early Warning*, Myers, R.F., Ed., Springer, 2011, pp. 447–461.
- Kanamori, H., The energy release in great earthquakes, *J. Geophys. Res.*, 1977, pp. 2981–2987.
- Kanamori, H. and Polet, Y., Tsunami earthquakes, in *Encyclopedia of Complexity and Systems Science*, Myers, R., Ed., Springer, 2007, pp. 9577–9592.
- Lee, J., Friederich, W., and Meier, T., Real time monitoring of moment magnitude by waveform inversion, *Geophys. Res. Lett.*, 2012, vol. 39, no. 2, L02309. doi 10.1029/2011GL050210
- Okal, E.A. and Talandier, J.,  $M_m$ : A variable period mantle magnitude, *J. Geophys. Res.*, 1989, vol. 94, pp. 4169–4193.
- Prozorov, A., Shimshoni, M., and Knopoff, L., Magnitude studies from ultra-long-period records, *Geophys. J. Int.*, 1977, vol. 48, no. 3, pp. 407–414.
- Schindelé, F., Reymond, D., Gaucher, E., and Okal, E.A., Analysis and automatic processing in near-field of the eight 1992–1994 tsunamigenic earthquakes: Improvements in real-time tsunami warning, *Pure Appl. Geophys.*, 1995, vol. 144, pp. 381–408.
- Talandier, J. and Okal, E.A., One-station estimates of seismic moments from the mantle magnitude  $M_m$ : The case of the regional field ( $1.5^\circ \leq \Delta \leq 15^\circ$ ), *Pure Appl. Geophys.*, 1992, vol. 138, pp. 3–60.
- Tsuboi, S.K., Abe, K., Takano, K., and Yamanaka, Y., Rapid determination of  $M_w$  from broadband  $P$ -wave forms, *Bull. Seismol. Soc. Am.*, 1995, vol. 83, pp. 606–613.
- Vanek, I., Zatopek, A., Karnik, V., Kondorskaya, N.V., Riznichenko, Yu.V., Savarenskii, E.F., Solov'ev, S.L., and Shebalin, N.V., Standard magnitude scale, *Izv. Akad. Nauk SSSR, Ser. Geofiz.*, 1962, no. 2, pp. 153–158.

Translated by V. Arutyunyan